Comparison of experimental and theoretical electron-impact-ionization triple-differential cross sections for ethane

Esam Ali,[1,*] Kate Nixon,[2,3] Andrew Murray,[2] Chuangang Ning,[4] James Colgan,[5] and Don Madison[1]

[1]*Department of Physics, Missouri University of Science and Technology, Rolla Missouri 65409, USA*

[2]*Photon Science Institute, School of Physics & Astronomy, University of Manchester, Manchester M13 9PL, United Kingdom*

[3]*School of Biology, Chemistry and Forensic Science, University of Wolverhampton, Wolverhampton WVl lLY, United Kingdom*

[4]*Department of Physics, State Key Laboratory of Low-Dimensional Quantum Physics, Tsinghua University, Beijing 100084, China*

[5]*Theoretical Division, Los Alamos National Laboratory, Los Alamos, New Mexico 87545, USA*

(Received 31 August 2015; published 30 October 2015)

We have recently examined electron-impact ionization of molecules that have one large atom at the center, surrounded by H nuclei (H_2O, NH_3, CH_4). All of these molecules have ten electrons; however, they vary in their molecular symmetry. We found that the triple-differential cross sections (TDCSs) for the highest occupied molecular orbitals (HOMOs) were similar, as was the character of the HOMO orbitals which had a *p*-type "peanut" shape. In this work, we examine ethane (C_2H_6) which is a molecule that has two large atoms surrounded by H nuclei, so that its HOMO has a double-peanut shape. The experiment was performed using a coplanar symmetric geometry (equal final-state energies and angles). We find the TDCS for ethane is similar to the single-center molecules at higher energies, and is similar to a diatomic molecule at lower energies.

DOI: 10.1103/PhysRevA.92.042711 PACS number(s): 34.80.Gs, 34.50.Ez, 34.10.+x

I. INTRODUCTION

Studies of electron-impact ionization of atoms and molecules play an important role for understanding the dynamical collisions of few-body systems. For the most elementary three-body problems, namely, electron-impact ionization of atomic hydrogen and helium, the convergent close-coupling (CCC) method [1], the time-dependent close-coupling (TDCC) method [2], and the exterior complex scaling (ECS) technique [3] provide essentially exact results. A similarly accurate theory is, however, lacking for the larger atoms and molecules. Very recently, the *b*-spline *R* matrix with pseudostates (BSR) and three-body distorted wave (3DW) approaches were shown to yield very good agreement with relatively absolute (ratios of cross sections are absolute) three-dimensional (3D) measurements for 64 eV electron-impact ionization of Ne [4].

The distorted wave approach is the most versatile theoretical method since it can be applied with equal ease to atoms and molecules, and the molecular three-body distorted wave (M3DW) approximation has been shown to give reasonably accurate results for ionization of several molecules.

There have been many high-energy studies of electron-impact ionization of molecules. These greatly enhance our understanding of molecular wave functions, since in the high-energy collisions the measured cross section is proportional to the momentum space wave function. More recently, low-energy studies from molecules have begun to be reported. These studies are much more difficult for theory, since the cross sections are strongly dependent on the dynamics of the ionizing interaction. Initial studies were for the ionization of simple diatomic and triatomic molecules such as H_2 [5–10], N_2 [11–14], N_2O [15], CO_2 [14,16], and H_2O [17–19]. More recently larger molecular targets such as CH_4 [20–23], NH_3 [24], formic acid [25], and DNA analogs such as phenol, pyrimidine, and tetrahydrofuran among others [26–32] have been studied. Our previous studies on the isoelectronic series of H_2O [18], NH_3 [24], and CH_4 [22,23], each containing ten electrons, have been particularly insightful as they were all conducted in a similar energy regime and under the same kinematics. This allowed us to observe trends in the data across the molecular series. Also, all of these molecules have a large nucleus at, or near, the center of mass (CM) that is surrounded by lighter H nuclei. By contrast the symmetry of the molecular frame is different in each case; i.e., H_2O is planar, NH_3 is pyramidal, and CH_4 is tetrahedral. At the low energies used in these studies, it is expected that the ionization process will be dominated by the dynamics of the collision. Indeed, the measured triple-differential cross sections (TDCSs) for all of these molecular targets were found to be similar. Notwithstanding this, the influence of the orbital character could still be observed in the measured TDCS. The measured cross sections were found to be similar when scattering from target orbitals of the same character, that is, having *s*-like or *p*-like character, regardless of the target. This observation implies that the spatial arrangement of the atoms, or molecular symmetry, does not have a large effect on the ionization dynamics. Further, it was observed that the theoretical predictions did not show this variation with orbital character, suggesting that they are not sensitive to the character of the orbital. One suggestion to explain this observation in the experimental data is that the H atoms are light and may not contribute much to the scattering mechanism. The purpose of this work is hence to examine a molecule with two large nuclei which are similarly surrounded by lighter nuclei, to ascertain if the cross sections are similar to molecules such as H_2O, CH_4, or NH_3, or if they are similar to those of diatomic molecules. We can also observe the trends in the theoretical predictions to ascertain if they are influenced by the quasidiatomic nature of such a molecule. For this study, we have chosen the ethane molecule (C_2H_6), which is a relatively small molecule that has two large carbon nuclei and six light hydrogen nuclei.

*Corresponding author: eaagx2@mst.edu

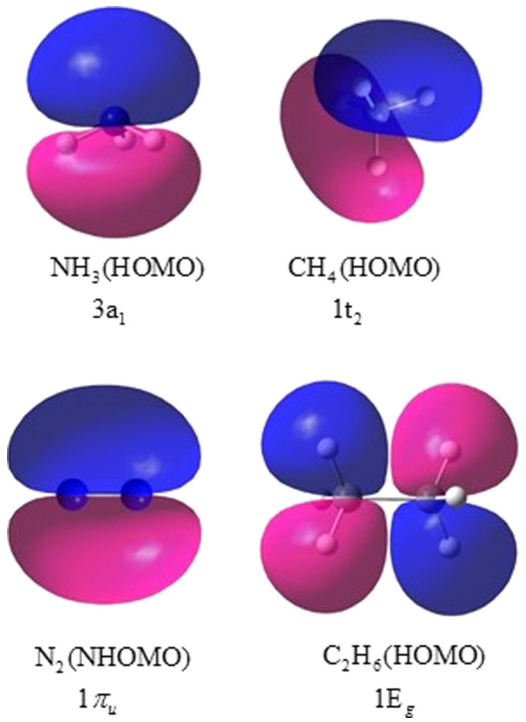

FIG. 1. (Color online) Dyson orbitals calculated for NH_3, CH_4, N_2, and C_2H_6.

Figure 1 compares the HOMO Dyson orbital for C_2H_6 with that for NH_3 and CH_4, both of which have a single large atom near the CM. As can be seen, the HOMO orbitals for these molecules are both p type, showing a characteristic "peanut" shape. Also shown is the next highest-occupied molecular orbital (NHOMO) for the diatomic molecule N_2, since it also has this shape. While the orbitals for NH_3, CH_4, and N_2 are all p type in character, C_2H_6 has a *double* p-type shape. From these orbitals, all of which exhibit p-like character, the obvious question is whether the cross section from ethane shows the same characteristics as the previous molecules with a single large atom near the center of mass, or if the presence of the two large atoms within the molecule modifies the scattering dynamics yielding a cross section similar to a diatomic molecule, or if the double p-type shape produces a totally different TDCS.

Theoretically it was found that the M3DW coupled with the orientation averaged molecular orbital (OAMO) approximation yielded qualitative agreement with experimental data for ionization of H_2O [18], NH_3 [24], and CH_4 [22,23]. However, a calculation doing a proper average (PA) over all orientations for CH_4 yielded much improved agreement with experimental data compared to the OAMO results [33]. Here we will compare experimental results for ethane with both M3DW-OAMO and PA results.

The experimental measurements were made using a coplanar symmetric geometry as shown in Fig. 2. In this geometry, both final-state electrons are detected in the scattering plane with $E_a = E_b$ and $\theta_a = \theta_b$ where E_a is the energy of the scattered electron with momentum $\mathbf{k}_a$ observed at scattering angle θ_a, and E_b is the energy of the ejected electron with momentum $\mathbf{k}_b$ observed at scattering angle θ_b. Obviously the

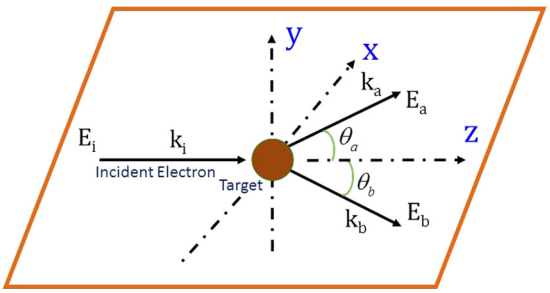

FIG. 2. (Color online) Coplanar symmetric geometry used for experimental measurements. See text for definition of the different variables.

electrons cannot be distinguished, but for convenience we call one of the electrons the scattered projectile and the other the ejected electron. From energy conservation the binding energy (ε) is given by

$$\varepsilon = E_i - E_a - E_b, \tag{1}$$

where E_i is the energy of the incoming electron with momentum $\mathbf{k}_i$.

In this paper we report experimental and theoretical results for electron-impact $(e,2e)$ ionization of the HOMO orbital of the ethane molecule (C_2H_6) in coplanar symmetric scattering for four final-state electron energies $E_a = E_b =$ 5, 10, 15, and 20 eV. We also compare the experimental ethane cross sections with those for CH_4, NH_3, and N_2. The experimental cross sections are then compared with theoretical M3DW calculations.

II. EXPERIMENT

The experimental data collected at the University of Manchester utilized a computer controlled and computer optimized $(e,2e)$ spectrometer. This spectrometer has been fully described elsewhere [34]; however, the relevant details are again briefly given here for completeness. The incident electron beam is produced by an electron gun which uses a tungsten filament cathode and two three-element aperture lenses to transport and accelerate the electrons into a well collimated beam of the desired energy. The electron beam is crossed with the molecular target (high-purity ethane, BOC [35]) effusing from a gas jet. The flow or ethane was controlled by a needle valve such that typical operating pressures were 1×10^{-5} Torr. The outgoing electrons, resulting from a collision with the molecular target, are collected by two analyzers, each consisting of a three-element lens and hemispherical energy selector. The transmitted electrons are detected by a channel electron multiplier. Each analyzer is mounted on an individual turntable that enables them to rotate independently around the detection plane over the angles of $35^\circ < \theta < 125^\circ$. To ensure that the spectrometer remained optimized over the time of data collection, the electrostatic lenses in the apparatus were adjusted under computer control as the experiment progressed, so as to maximize the electron count rate in each analyzer. This corrected for any variation in the signals as the analyzers swept back and forth around the detection plane. The experimental data reported here are

an average of several sweeps around the detection plane with the uncertainty being the standard error for the average at each particular angle. The uncertainty on the analyzer angle is estimated to be $\sim 3^\circ$ with contributions from the pencil angle of the incident electron beam and the acceptance angle of the analyzers. The coincidence energy resolution obtained in this study is $\sim$0.9 eV, as determined by the binding energy spectrum of helium.

III. THEORY

The molecular three-body distorted wave (M3DW) approximation is described in Refs. [36,37] and here we provide only a short review. The triple-differential cross section (TDCS) is given by

$$\frac{d^5\sigma}{d\Omega_a d\Omega_b dE_b} = \frac{1}{(2\pi)^5}\frac{k_a k_b}{k_i}(|T_{\rm dir}|^2 + |T_{\rm exc}|^2 + |T_{\rm dir} - T_{\rm exc}|^2), \tag{2}$$

where $\mathbf{k}_i$, $\mathbf{k}_a$, and $\mathbf{k}_b$ are the wave vectors for the initial, scattered, and ejected electrons, respectively; $T_{\rm dir}$ is the direct scattering amplitude; and $T_{\rm exc}$ is the exchange amplitude. The direct scattering amplitude is given by

$$T_{\rm dir} = \langle \chi_a^-(\mathbf{k}_a,\mathbf{r}_0)\chi_b^-(\mathbf{k}_b,\mathbf{r}_1)C_{ab}(\mathbf{r}_{01})\psi_{\rm Ion}(\xi,\mathbf{R}) \times |V_i - U_i|\psi_{\rm Target}(\xi,\mathbf{r}_1,\mathbf{R})\chi_i^+(\mathbf{k}_i,\mathbf{r}_0)\rangle, \tag{3}$$

where $\chi_i^+(\mathbf{k}_i,\mathbf{r}_0)$ is a continuum-state distorted for wave number k_i and the (+) indicates outgoing wave boundary conditions; $\chi_a^-(\mathbf{k}_a,\mathbf{r}_0)$, $\chi_b^-(\mathbf{k}_b,\mathbf{r}_1)$ are the scattered and ejected electron distorted waves with incoming wave boundary conditions; the factor $C_{ab}(\mathbf{r}_{01})$ is the final-state Coulomb-distortion factor between the two electrons—normally called postcollision interaction (PCI), $\psi_{\rm Target}(\xi,\mathbf{r}_1,\mathbf{R})$ is the initial-state molecular wave function which depends on the orientation of the molecule $\mathbf{R}$, the active electron $\mathbf{r}_1$, and all the passive electrons ξ; and finally $\psi_{\rm Ion}(\xi,\mathbf{R})$ is the final-state ion wave function which depends on the orientation and on the passive electrons. In the approximation we use for the perturbation $(V_i - U_i)$, this only depends on the projectile electron (r_0) and active electron (r_1). Since the perturbation does not depend on the passive electron coordinates ξ, we can integrate over all these coordinates and define

$$\phi_{Dy}(\mathbf{r}_1,\mathbf{R}) = \langle \psi_{\rm Ion}(\xi,\mathbf{R})|\psi_{\rm Target}(\xi,\mathbf{r}_1,\mathbf{R})\rangle. \tag{4}$$

Here $\phi_{Dy}(\mathbf{r}_1,\mathbf{R})$ is the initial bound-state wave function which is commonly called the Dyson molecular orbital for the active electron, which depends both on $\mathbf{r}_1$ and $\mathbf{R}$. Defining the perturbation to be W, we have

$$T_{\rm dir}(\mathbf{R}) = \langle \chi_a^-(\mathbf{k}_a,\mathbf{r}_0)\chi_b^-(\mathbf{k}_b,\mathbf{r}_1)C_{ab}(\mathbf{r}_{01}) \times |W|\phi_{Dy}(\mathbf{r}_1,\mathbf{R})\chi_i^+(\mathbf{k}_i,\mathbf{r}_0)\rangle. \tag{5}$$

The exchange T matrix is the same as Eq. (5) except that $\mathbf{r}_0$ and $\mathbf{r}_1$ are interchanged in the final-state wave function. The triple-differential cross section (TDCS) for a given orientation $\mathbf{R}$ with respect to the laboratory frame can be obtained from

$$\sigma^{\rm TDCS}(\mathbf{R}) = \frac{1}{(2\pi)^5}\frac{k_a k_b}{k_i}[|T_{\rm dir}(\mathbf{R})|^2 + |T_{\rm exc}(\mathbf{R})|^2 + |T_{\rm dir}(\mathbf{R}) - T_{\rm exc}(\mathbf{R})|^2]. \tag{6}$$

A. Proper average (PA) over molecular orientations

To take the proper average (PA) over all molecular orientations, the TDCS is calculated for each orientation and then averaged over all possible orientations so that

$$\sigma^{\rm PA} = \frac{\int \sigma^{\rm TDCS}(\mathbf{R})d\Omega_R}{\int d\Omega_R}. \tag{7}$$

Looking only at the direct scattering amplitude as an example, this leads to

$$\sigma^{\rm PA} = \frac{\int \frac{1}{(2\pi)^5}\frac{k_a k_b}{k_i}\left|\int d^3r_0 d^3r_1 \chi_a^{-*}(\mathbf{k}_a,\mathbf{r}_0)\chi_b^{-*}(\mathbf{k}_b,\mathbf{r}_1)C_{ab}(\mathbf{r}_{01})W(\mathbf{r}_0,\mathbf{r}_1)\phi_{Dy}(\mathbf{r}_1,\mathbf{R})\chi_i^+(\mathbf{k}_i,\mathbf{r}_0)\right|^2 d\Omega_R}{\int d\Omega_R}. \tag{8}$$

B. OAMO approximation

In the OAMO (orientation averaged molecular orbital) approximation [36], we assume that the absolute value and integral over molecular orientations in Eq. (8) commute, so that

$$\sigma^{\rm OAMO} \simeq \frac{1}{(2\pi)^5}\frac{k_a k_b}{k_i}\frac{\left|\int d\Omega_R\left\{\int d^3r_0 d^3r_1 \chi_a^{-*}(\mathbf{k}_a,\mathbf{r}_0)\chi_b^{-*}(\mathbf{k}_b,\mathbf{r}_1)C_{ab}(\mathbf{r}_{01})W(\mathbf{r}_0,\mathbf{r}_1)\phi_{Dy}(\mathbf{r}_1,\mathbf{R})\chi_i^+(\mathbf{k}_i,\mathbf{r}_0)\right\}\right|^2}{\int d\Omega_R}. \tag{9}$$

Since the only term in the integral that depends on the orientation is the Dyson orbital, we can interchange the order of integration, so that

$$\sigma^{\rm OAMO} \simeq \frac{1}{(2\pi)^5}\frac{k_a k_b}{k_i}\frac{\left|\int d^3r_0 d^3r_1 \chi_a^{-*}(\mathbf{k}_a,\mathbf{r}_0)\chi_b^{-*}(\mathbf{k}_b,\mathbf{r}_1)C_{ab}(\mathbf{r}_{01})W(\mathbf{r}_0,\mathbf{r}_1)\int \phi_{Dy}(\mathbf{r}_1,\mathbf{R})d\Omega_R\chi_i^+(\mathbf{k}_i,\mathbf{r}_0)\right|^2}{\int d\Omega_R}. \tag{10}$$

We now define the OAMO Dyson wave function,

$$\phi_{Dy}^{\rm OAMO}(\mathbf{r}_1) = \frac{\int \phi_{Dy}(\mathbf{r}_1,\mathbf{R})d\Omega_R}{\int d\Omega_R}, \tag{11}$$

so that

$$\sigma^{\mathrm{OAMO}} = \frac{1}{(2\pi)^5}\frac{k_a k_b}{k_i}\left|\int d^3r_0 d^3r_1 \chi_a^{-*}(\mathbf{k}_a,\mathbf{r}_0)\chi_b^{-*}(\mathbf{k}_b,\mathbf{r}_1)C_{ab}(\mathbf{r}_{01})W(\mathbf{r}_0,\mathbf{r}_1)\phi_{Dy}^{\mathrm{OAMO}}(\mathbf{r}_1)\chi_i^{+}(\mathbf{k}_i,\mathbf{r}_0)\right|^2. \quad (12)$$

This is a T matrix just like one we would evaluate for ionization of an atom, or for ionization of a single molecular orientation. The advantage of this approximation is that this calculation does not take much computer time. By contrast, the PA calculation can take an enormous amount of computer time, depending on the number of orientations required for suitable convergence.

IV. RESULTS

In Fig. 3 we compare the present experimental ethane cross sections with previously published data for CH_4 [22], NH_3 [24], and N_2 [12]. As absolute data have not been measured, each of the data sets is normalized to unity at its most intense point. From the figure, it is seen that the TDCS measurements are similar for all four molecules at the two highest energies of 20 and 15 eV. All of them show high intensity at low angles, a minimum at $\theta \sim 90°$ followed by the cross section increasing again at high analyzer angles. A signature of a p-like orbital observed in the isoelectronic targets is a small "dip" in the large peak at low angles which is also present in the ethane data, but less obvious in N_2. By contrast, at 10 and 5 eV ethane shows a very different character from the two molecules that have a single heavy atom near the CM. At 10 eV ethane is very similar to the diatomic molecule N_2, and at 5 eV ethane is quasi-isotropic and therefore different from all the other measurements. These observations suggest that for the higher energies, the incoming electron scatters from one of the peanut-like orbitals, with very little influence from the second orbital, or the diatomic nature of the molecule. As the energy is lowered to 10 eV, the results look more like a diatomic molecule, suggesting that the outer six H nuclei do not play an important role but that the two-center nature of the target influences the dynamics. As the energy is further lowered to 5 eV, it appears that the interactions become much more complicated and the data cannot be explained by these simple ideas.

Figure 4 compares experimental and theoretical results for electron-impact ionization of ethane. Both the data and theoretical calculations have been normalized to unity at their largest values. The solid (red) curves are the proper average (PA) results and the dashed (blue) curves are the OAMO

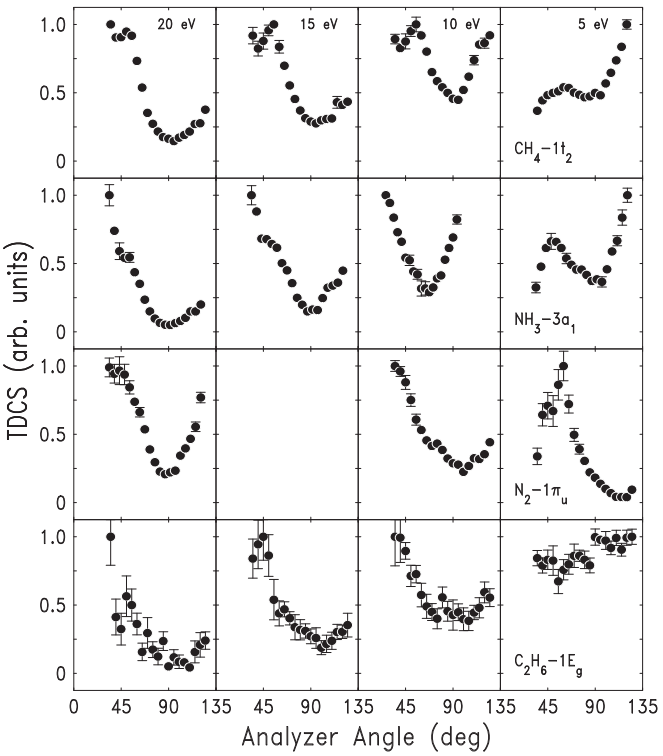

FIG. 3. Experimental TDCS for coplanar symmetric electron-impact ionization of NH_3, CH_4, N_2, and C_2H_6 as a function of electron detection angle, for a series of outgoing electron energies. Both final-state electrons have equal energies as listed in the top row, and both are detected at equal angles as shown in Fig. 2. For each set of energies, the largest measured data have been normalized to unity.

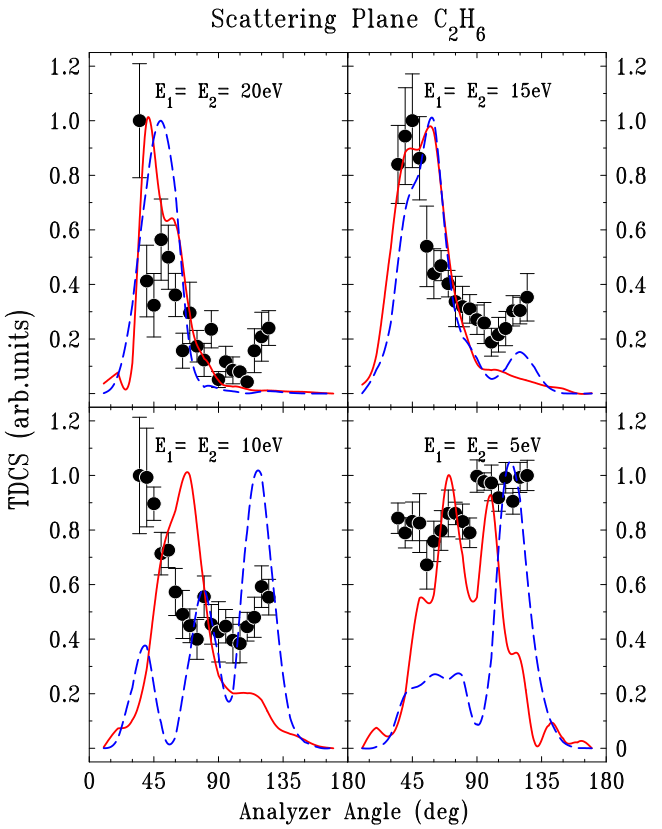

FIG. 4. (Color online) Experimental and theoretical TDCS for electron-impact ionization of ethane (C_2H_6) as a function of electron detection angle, using the geometry in Fig. 2. For both experimental data and theoretical calculations, the largest cross sections have been normalized to unity for each set of energies. The theoretical curves are solid (red) is PA and dashed (blue) is OAMO.

results. For the highest energies of 15 and 20 eV, there is qualitative agreement between experiment and theory for the small angle peak. For 20 eV, the PA results are in somewhat better agreement with experiment than the OAMO calculation, in that the location of the forward peak is closer to the data, and also shows a dip in this peak. At 15 eV, both theories have small angle peaks which have shifted to larger scattering angles. Since both PA and OAMO have the exact electron-electron PCI repulsion, this shift suggests that the theoretical repulsion is stronger than observed. There is a second large angle peak at high scattering angles in the experimental data that is present in the OAMO theory but is not predicted by the PA calculations.

For the two lowest energies, the agreement between experiment and theory is less satisfactory. At 10 eV, the OAMO predicts three peaks, which is similar to the data. However, the first peak is much too small and the third one appears to be too big. The PA, on the other hand, has a single small angle peak. Unfortunately, the PA peak is shifted to a much larger angle than is found in the experiment. While the experimental data show a second peak for large angles, the PA calculation only shows a shoulder in this angular range. The lack of a significant large angle peak for 15 and 10 eV may indicate that the nuclear scattering is underestimated in the PA model since it has been previously found that a strong interaction with the nucleus is necessary to obtain both outgoing electrons at large angles [9]. At 5 eV, the data shows little variation with angle, unlike the theoretical results. However, the data appear to have (at least) three peaks in this angular range which is also predicted by the PA calculation. The PA results are an improvement over that of the OAMO, in that OAMO predicts a single narrow peak at large angles while the PA predicts multiple peaks of comparable heights, similar to the data.

V. CONCLUSIONS

We have presented experimental and theoretical results for electron-impact ionization from the ethane (C_2H_6) HOMO for coplanar symmetric scattering. Both electrons in the final state have equal energies and are detected at equal angles on opposite sides of the incident beam direction. Four different final-state energies between 5 and 20 eV have been examined.

Ethane can be considered as a quasidiatomic molecule of C_2 surrounded by six H nuclei, and the HOMO looks like two p-type "peanut" states side by side. We have compared the experimental measurements with equivalent data for electron-impact ionization of NH_3 and CH_4, which have a p-type HOMO state with one large atom near the CM surrounded by H nuclei. We also compared with experimental data for the NHOMO state of N_2. N_2 is of course not surrounded by H nuclei, but has the same two heavy atom molecular frame and, further, its NHOMO orbital also has a peanut shape. We found that at the two highest energies of 15 and 20 eV, the cross sections for all four molecules were similar, suggesting that the projectile electron scatters from one of the ethane orbitals with little influence from the second. At 10 eV, the ethane results were quite different from NH_3 and CH_4 but were similar to N_2. This suggests that as the energy is lowered, the electron "sees" an effective diatomic molecule with little influence from the surrounding H nuclei. At the lowest energy of 5 eV, the ethane data were different to any of the other three molecules (but closest to N_2), suggesting that the scattering process is more complicated.

We also compared the ethane experimental data with theoretical M3DW results calculated using both the OAMO approximation and a proper average (PA) over all orientations. For the highest energy of 20 eV, the PA results were in reasonable agreement with experiment for the small angle peak, while at 15 and 10 eV the agreement was more qualitative, with the theoretical peak shifting to increasingly larger angles as the energy decreases. For 5 eV, the PA calculation was again in qualitative agreement with experiment. In all cases, the PA results agreed with experimental data more closely than the OAMO results, as would be expected.

ACKNOWLEDGMENTS

K.N. would like to thank the European commission for a Marie Curie International Incoming Fellowship undertaken at the University of Manchester. We would like to thank the technicians in the Schuster laboratory for providing excellent support for the experimental apparatus. This work was partly supported by the US National Science Foundation under Grant No. PHY-1505819 and by the National Natural Science Foundation of China under Grant No. 11174175. Computational work was performed with Institutional Computing resources made available through the Los Alamos National Laboratory and XSEDE resources provided by the Texas Advanced Computing Center (Grant No. TG-MCA07S029). The Los Alamos National Laboratory is operated by Los Alamos National Security, LLC, for the National Nuclear Security Administration of the US Department of Energy under Contract No. DE-AC5206NA25396.

[1] I. Bray and A. T. Stelbovics, Phys. Rev. A **46**, 6995 (1992).
[2] J. Colgan and M. S. Pindzola, Phys. Rev. A **74**, 012713 (2006).
[3] T. N. Rescigno, M. Baertschy, W. A. Isaacs, and C. W. McCurdy, Science **286**, 2474 (1999).
[4] X. Ren, S. Amami, O. Zatsarinny, T. Pfluger, M. Weyland, W. Y. Baek, H. Rabus, K. Bartschat, D. Madison, and A. Dorn, Phys. Rev. A **91**, 032707 (2015).
[5] A. Senftleben, T. Pflueger, X. Ren, O. Al-Hagan, B. Najjari, D. Madison, A. Dorn, and J. Ullrich, J. Phys. B **43**, 081002 (2010).
[6] D. S. Milne-Brownlie, M. Foster, J. Gao, B. Lohmann, and D. H. Madison, Phys. Rev. Lett. **96**, 233201 (2006).
[7] A. J. Murray, J. Phys. B **38**, 1999 (2005).
[8] E. M. Staicu Casagrande, A. Naja, F. Mezdari, A. Lahmam-Bennani, P. Bolognesi, B. Joulakian, O. Chuluunbaatar, O. Al-Hagan, D. H. Madison, D. V. Fursa, and I. Bray, J. Phys. B **41**, 025204 (2008).
[9] O. Al-Hagan, C. Kaiser, D. H. Madison, and A. J. Murray, Nat. Phys. **5**, 59 (2009).

[10] J. Gao, D. H. Madison, J. L. Peacher, A. J. Murray, and M. J. Hussey, J. Chem. Phys. **124**, 194306 (2006).
[11] A. J. Murray, M. J. Hussey, I. Bray, J. Gao, and D. H. Madison, J. Phys. B **39**, 3945 (2006).
[12] M. J. Hussey and A. J. Murray, J. Phys. B **35**, 3399 (2002).
[13] L. R. Hargreaves, C. Colyer, M. A. Stevenson, B. Lohmann, O. Al-Hagan, D. H. Madison, and C. G. Ning, Phys. Rev. A **80**, 062704 (2009).
[14] A. Lahmam-Bennani, E. M. Staicu Casagrande, and A. Naja, J. Phys. B **42**, 235205 (2009).
[15] S. J. Cavanagh and B. Lohmann, J. Phys. B **32**, L261 (1999).
[16] M. J. Hussey and A. J. Murray, J. Phys. B **38**, 2965 (2005).
[17] D. S. Milne-Brownlie, S. J. Cavanagh, B. Lohmann, C. Champion, P. A. Hervieux, and J. Hanssen, Phys. Rev. A **69**, 032701 (2004).
[18] K. L. Nixon, A. J. Murray, O. Al-Hagan, D. H. Madison, and C. Ning, J. Phys. B **43**, 035201 (2010).
[19] C. Kaiser, D. Spieker, J. Gao, M. Hussey, A. Murray, and D. H. Madison, J. Phys. B **40**, 2563 (2007).
[20] A. Lahmam-Bennani, A. Naja, E. M. Staicu Casagrande, N. Okumus, C. Dal Cappello, I. Charpentier, and S. Houamer, J. Phys. B **42**, 165201 (2009).
[21] S. Xu, H. Chaluvadi, X. Ren, T. Pflüger, A. Senftleben, C. G. Ning, S. Yan, P. Zhang, J. Yang, X. Ma, J. Ullrich, D. H. Madison, and A. Dorn, J. Chem. Phys. **137**, 024301 (2012).
[22] K. L. Nixon, A. J. Murray, H. Chaluvadi, C. G. Ning, and D. H. Madison, J. Chem. Phys. **134**, 174304 (2011).
[23] K. L. Nixon, A. J. Murray, H. Chaluvadi, S. Amami, D. H. Madison, and C. G. Ning, J. Chem. Phys. **136**, 094302 (2012).
[24] K. L. Nixon, A. J. Murray, H. Chaluvadi, C. G. Ning, J. Colgan, and D. H. Madison, J. Chem. Phys. **138**, 174304 (2013).
[25] C. J. Colyer, M. A. Stevenson, O. Al-Hagan, D. H. Madison, C. G. Ning, and B. Lohmann, J. Phys. B **42**, 235207 (2009).
[26] J. D. Builth-Williams, S. M. Bellm, L. Chiari, P. A. Thorn, D. B. Jones, H. Chaluvadi, D. H. Madison, C. G. Ning, B. Lohmann, G. B. da Silva, and M. J. Brunger, J. Chem. Phys. **139**, 034306 (2013).
[27] D. B. Jones, J. D. Builth-Williams, S. M. Bellm, L. Chiari, H. Chaluvadi, D. H. Madison, C. G. Ning, B. Lohmann, O. Ingolfsson, and M. J. Brunger, Chem. Phys. Lett. **572**, 32 (2013).
[28] S.M. Bellm, J. D. Builth-Williams, D. B. Jones, H. Chaluvadi, D. H. Madison, C. G. Ning, F. Wang, X. G. Ma, B. Lohmann, and M. J. Brunger, J. Chem. Phys. **136**, 244301 (2012).
[29] S.M. Bellm, C. J. Colyer, B. Lohmann, and C. Champion, Phys. Rev. A **85**, 022710 (2012).
[30] J. D. Builth-Williams, S. M. Bellm, D. B. Jones, H. Chaluvadi, D. H. Madison, C. G. Ning, B. Lohmann, and M. J Brunger, J. Chem. Phys. **136**, 024304 (2012).
[31] C. J. Colyer, S. M. Bellm, B. Lohmann, G. F. Hanne, O. Al-Hagan, D. H. Madison, and C. G. Ning, J. Chem. Phys. **133**, 124302 (2010).
[32] G. B. da Silva, R. F. C. Neves, L. Chiari, D. B. Jones, E. Ali, D. H. Madison, C. G. Ning, K. L. Nixon, M. C. A. Lopes, and M. J. Brunger, J. Chem. Phys. **141**, 124307 (2014).
[33] H. Chaluvadi, C. G. Ning, and D. Madison, Phys. Rev. A **89**, 062712 (2014).
[34] A. J. Murray, B. C. H. Turton, and F. H. Read, Rev. Sci. Instrum. **63**, 3346 (1992).
[35] BOC Industrial Gases UK, http://www.boconline.co.uk.
[36] J. Gao, J. L. Peacher, and D. H. Madison, J. Chem. Phys. **123**, 204302 (2005).
[37] D. H. Madison and O. Al-Hagan, J. At., Mol., Opt. Phys. **2010**, 367180 (2010).